

At present, the output power is low because of the narrow gate width of the GaAs FET used. However, an output power of 1 W or more is obtainable with improvements in the device in the future. The features described indicate that the GaAs FET oscillator will soon be joining the family of microwave solid-state oscillators as a promising new member.

ACKNOWLEDGMENT

The authors wish to thank H. Yoshine and M. Nagata for encouragement to perform this work.

REFERENCES

- [1] C. A. Liechti, E. Gowen, and J. Cohen, "GaAs microwave Schottky-gate field-effect transistor," in *1972 ISSCC Dig. Tech. Papers*, pp. 158-159, Feb. 1972.
- [2] W. Baechtold *et al.*, "Si and GaAs 0.5 μ m-gate Schottky-barrier field-effect transistors," *Electron. Lett.*, vol. 9, pp. 232-234, May 1973.
- [3] C. A. Liechti and R. L. Tillman, "Design and performance of microwave amplifiers with GaAs Schottky-gate field-effect transistors," *IEEE Trans. Microwave Theory Tech.*, vol. MTT-22, pp. 510-517, May 1974.
- [4] W. Baechtold, "X- and Ku-band amplifiers with GaAs Schottky-barriers field-effect transistors," *IEEE J. Solid-State Circuits (Special Issue on Microwave Integrated Circuits)*, vol. SC-8, pp. 54-58, Feb. 1973.
- [5] "A practical 4 to 8 GHz GaAs FET amplifier," *Microwave J.*, vol. 17, p. 26, Feb. 1974.
- [6] J. E. Sitch and P. N. Robson, "The performance of GaAs field-effect transistors as microwave mixers," *Proc. IEEE (Lett.)*, vol. 61, pp. 399-400, Mar. 1973.
- [7] M. Maeda, S. Takahashi, and H. Kodera, "CW oscillation characteristics of GaAs Schottky-barrier gate field-effect transistors," *Proc. IEEE (Lett.)*, vol. 63, pp. 320-321, Feb. 1975.
- [8] S. Okazaki *et al.*, "Microwave oscillation with GaAs FET," presented at 6th Conf. Solid State Devices, Tokyo, Japan, Aug. 1974.
- [9] S. Asai *et al.*, "Single- and dual-gate GaAs Schottky-barrier FET's for microwave frequencies," *Suppl. J. Jap. Soc. Appl. Phys.*, vol. 43, pp. 442-447, 1974.
- [10] J. Gonda, "Large signal transistor oscillator design," in *1972 IEEE G-MTT Int. Microwave Symp. Dig. Tech. Papers*, pp. 110-112, May 1972.
- [11] J. W. Gewartowski, "The effect of series resistance on avalanche diode (IMPATT) oscillator efficiency," *Proc. IEEE (Lett.)*, vol. 56, pp. 1139-1140, June 1968.
- [12] L. S. Napoli *et al.*, "High-power GaAs FET amplifier—A multi-gate structure," in *1973 ISSCC Dig. Tech. Papers*, pp. 82-83, Feb. 1973.
- [13] M. Fukuta *et al.*, "Mesh source type microwave power FET," *ibid.*, pp. 84-85, Feb. 1973.
- [14] J. Cohen and M. Gilden, "Temperature stability of an MIC Gunn-effect oscillator," *IEEE Trans. Microwave Theory Tech. (Short Papers)*, vol. MTT-21, pp. 115-116, Feb. 1973.
- [15] C. K. Chan and R. S. Cole, "A stable integrated circuit X-band Gunn oscillator," *IEEE Trans. Microwave Theory Tech. (Lett.)*, vol. MTT-22, p. 815, Aug. 1974.
- [16] J. Josenhans, "Noise spectra of Read diode and Gunn oscillators," *Proc. IEEE (Lett.)*, vol. 54, pp. 1478-1479, Oct. 1966.
- [17] J. R. Ashley and F. M. Palka, "Noise properties and stabilization of Gunn and avalanche diode oscillators and amplifiers," in *1970 IEEE G-MTT Int. Microwave Symp. Dig. Tech. Papers*, pp. 161-164, May 1970.
- [18] P. A. Levine, H. C. Huang, and H. Johnson, "Impatt shoot for Gunn noise levels," *Microwaves*, pp. 52-56, Apr. 1972.
- [19] M. Ohtomo, "Experimental evaluation of noise parameters in Gunn and avalanche oscillators," *IEEE Trans. Microwave Theory Tech.*, vol. MTT-20, pp. 425-437, July 1972.
- [20] K. P. Weller, "A study of millimeter-wave GaAs IMPATT oscillator and amplifier noise," *IEEE Trans. Electron Devices*, vol. ED-20, pp. 517-521, June 1973.

Harmonic Mixing with an Antiparallel Diode Pair

MARVIN COHN, FELLOW, IEEE, JAMES E. DEGENFORD, MEMBER, IEEE, AND BURTON A. NEWMAN, MEMBER, IEEE

Abstract—An analytical and experimental investigation of the properties of an antiparallel diode pair is presented. Such a configuration has the following unique and advantageous characteristics as a harmonic mixer: 1) reduced conversion loss by suppressing fundamental mixing products; 2) lower noise figure through suppression of local oscillator noise sidebands; 3) suppression of direct video detection; 4) inherent self protection against large peak inverse voltage burnout. These results are obtained without the use of either filters or balanced circuits employing hybrid junctions.

Manuscript received October 17, 1974; revised March 17, 1975. The authors are with the Electromagnetic Technology Laboratory, Westinghouse Defense and Space Center, Advanced Technology Laboratories, Baltimore, Md. 21203.

I. INTRODUCTION

HISTORICALLY harmonic mixing has been used primarily at the higher millimeter wave frequencies where reliable stable LO sources are either unavailable or prohibitively expensive. However, the conversion loss obtained by harmonic mixing has been typically 3 to 5 dB greater than that which could be obtained by fundamental mixing at the same signal frequency [1], [2]. An analysis [3], [4] has shown that such a large degradation should not exist, but it assumes that fundamental mixing between the signal and LO is suppressed. Fundamental mixing

will, however, take place unless the harmonic mixer provides a reactive termination for these mixer products. In general, that is difficult to accomplish, e.g., in the case of second-harmonic mixing the fundamental mixing difference frequency ($f_s - f_{LO}$) is close to the LO frequency.

In this paper, an analytical and experimental investigation of the properties of an antiparallel diode pair is presented [5]. Such a configuration has unique and advantageous characteristics as a harmonic generator or harmonic mixer. In the latter application, which is treated in this paper, it will be shown that this circuit provides:

- 1) reduced conversion loss by suppressing the fundamental mixing products;
- 2) lower noise figure through suppression of local oscillator noise sidebands;
- 3) suppression of direct video detection;
- 4) inherent self-protection against large peak inverse voltage burnout.

These results are obtained without the use of either filters or balanced circuits employing hybrid junctions.

II. ANALYSIS

In a conventional single diode mixer as shown in Fig. 1(a), application of a voltage waveform

$$V = V_{LO} \sin \omega_{LO} t + V_s \sin \omega_s t$$

to the usual asymmetric diode characteristic results in the diode current having all frequencies $m\omega_{LO} \pm nf_s$. It will be shown in this section that the total current of the antiparallel diode pair shown in Fig. 1(b) contains only frequencies for which $m + n$ is an odd integer. The terms in which $m + n$ is even, i.e., even harmonics, funda-

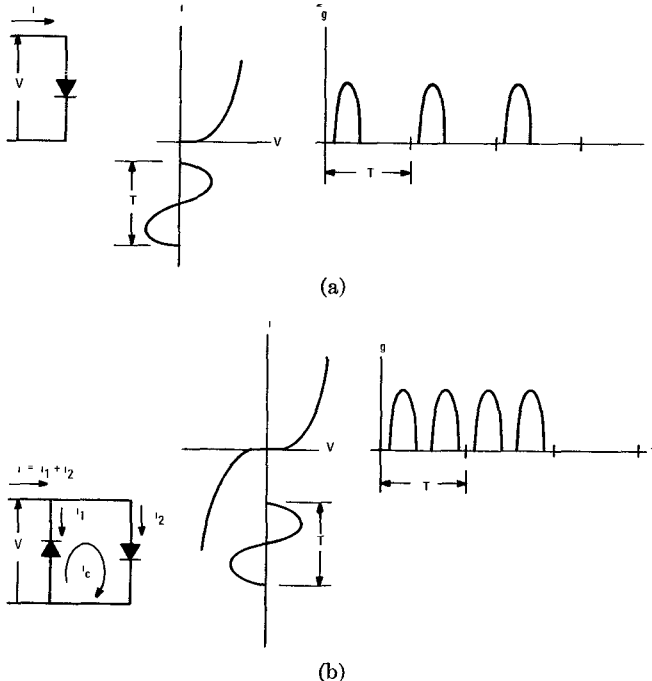


Fig. 1. Mixer circuit. (a) Single diode mixer. (b) Antiparallel diode pair mixer.

mental mixing products ($\omega_s - \omega_{LO}$ and $\omega_s + \omega_{LO}$), and the dc term flow only within the diode loop.

The basic antiparallel diode pair circuit is shown in Fig. 1(b). The instantaneous currents through the diodes i_1 and i_2 may be written in the usual fashion

$$i_1 = -i_s(e^{-\alpha V} - 1) \quad (1)$$

$$i_2 = i_s(e^{\alpha V} - 1) \quad (2)$$

where α is the diode slope parameter ($\alpha \approx 38 \text{ V}^{-1}$ for typical high-quality gallium arsenide Schottky barrier diodes). Similarly, the differential conductance for each diode may be written as

$$g_1 = \frac{di_1}{dV} = \alpha i_s e^{-\alpha V} \quad (3)$$

and

$$g_2 = \frac{di_2}{dV} = \alpha i_s e^{\alpha V}. \quad (4)$$

The composite time varying differential conductance g is simply the sum of the individual differential conductances.

$$\begin{aligned} g &= g_1 + g_2 = \alpha i_s (e^{\alpha V} + e^{-\alpha V}) \\ &= 2\alpha i_s \cosh \alpha V. \end{aligned} \quad (5)$$

Examination of this expression reveals that g has even symmetry with V and, as illustrated in Fig. 1(a) and (b), double the number of conductance pulses per LO cycle as compared to a single diode mixer.

For the usual case in which only the LO modulates the conductance of the diodes we may substitute

$$V = V_{LO} \cos \omega_{LO} t$$

into (5) with the following result

$$g = 2\alpha i_s \cosh (\alpha V_{LO} \cos \omega_{LO} t) \quad (6)$$

which may be expanded in the following series:

$$\begin{aligned} g &= 2\alpha i_s [I_0(\alpha V_{LO}) + 2I_2(\alpha V_{LO}) \cos 2\omega_{LO} t \\ &\quad + 2I_4(\alpha V_{LO}) \cos 4\omega_{LO} t + \dots] \end{aligned} \quad (7)$$

where $I_n(\alpha V_{LO})$ are modified Bessel functions of the second kind. Notice that the conductance components consist of a dc term plus even harmonics of the LO frequency, ω_{LO} . For the applied voltage, $V = V_{LO} \cos \omega_{LO} t + V_s \cos \omega_s t$, the current expression is

$$i = g(V_{LO} \cos \omega_{LO} t + V_s \cos \omega_s t) \quad (8)$$

$$\begin{aligned} i &= A \cos \omega_{LO} t + B \cos \omega_s t + C \cos 3\omega_{LO} t \\ &\quad + D \cos 5\omega_{LO} t + E \cos (2\omega_{LO} + \omega_s) t \\ &\quad + F \cos (2\omega_{LO} - \omega_s) t + G \cos (4\omega_{LO} + \omega_s) t \\ &\quad + H \cos (4\omega_{LO} - \omega_s) t + \dots \end{aligned} \quad (9)$$

It can be seen that the total current only contains frequency terms $m\omega_{LO} \pm nf_s$ where $m + n$ is an odd integer; i.e., $m + n = 1, 3, 5, \dots$

In Fig. 1(b) a circulating current i_c is also indicated.

This current arises from the fact that Fourier expansions of the individual currents i_1 and i_2 reveal that certain components of each current are oppositely phased. Because of their opposite polarity, these components cancel as far as the external current i is concerned and simply circulate within the loop formed by the two diodes. From Fig. 1, one can mathematically describe this circulating current as

$$\begin{aligned} i_c &= (i_2 - i_1)/2 \\ &= i_s[\cosh \alpha V - 1]. \end{aligned} \quad (10)$$

Substituting

$$V = V_{LO} \cos \omega_{LO} t + V_s \cos \omega_s t \quad (11)$$

into the expansion for the hyperbolic cosine yields

$$\begin{aligned} i_c &= i_s \left[1 + \frac{(V_{LO} \cos \omega_{LO} t + V_s \cos \omega_s t)^2}{2!} + \dots - 1 \right] \\ &= \frac{i_s}{2} [V_{LO}^2 \cos^2 \omega_{LO} t + V_s^2 \cos^2 \omega_s t + 2V_{LO}V_s \\ &\quad \cdot \cos \omega_{LO} t \cos \omega_s t + \dots] \quad (12) \\ &= \frac{i_s}{2} \left\{ \frac{V_{LO}^2 + V_s^2}{2} + \frac{V_{LO}^2}{2} \cos 2\omega_{LO} t + \frac{V_s^2}{2} \right. \\ &\quad \cdot \cos 2\omega_s t + V_{LO}V_s [\cos(\omega_{LO} - \omega_s)t \\ &\quad \left. + \cos(\omega_{LO} + \omega_s)t] + \dots \right\} \quad (13) \end{aligned}$$

from which it can be seen that the circulating current only contains frequencies $m\omega_0 \pm n\omega_s$, where

$$m + n = \text{even integer.} \quad (14)$$

Thus the antiparallel pair has the advantage of suppressing fundamental and other odd harmonic mixing products as well as even harmonics of the LO.

This natural suppression is lessened, of course, by diode unbalance. If we first consider the case where the saturation currents i_s are different for the two diodes, then we may let

$$i_{s1} = i_s + \Delta i_s \quad \text{and} \quad i_{s2} = i_s - \Delta i_s. \quad (15)$$

Substitution of the above expressions into (3), (4), and (5) yields the following equation for the total conductance g :

$$g = 2\alpha i_s \left[\cosh \alpha V + \frac{\Delta i_s}{i_s} \sinh \alpha V \right]. \quad (16)$$

Similarly, if the diode slope parameters are different, we may let

$$\alpha_1 = \alpha + \Delta \alpha \quad \text{and} \quad \alpha_2 = \alpha - \Delta \alpha \quad (17)$$

which yields the following expression for the total conductance:

$$g = 2\alpha i_s e^{(\Delta \alpha)V} \left[\cosh \alpha V + \frac{\Delta \alpha}{\alpha} \sinh \alpha V \right]. \quad (18)$$

Notice that in both cases, the conductance function contains the desired hyperbolic cosine term plus a hyperbolic sine term whose coefficient is proportional to either $\Delta i_s/i_s$ or $\Delta \alpha/\alpha$. This hyperbolic sine term introduces conductance variations at the fundamental and other odd harmonics of the LO. We may find the ratio of the conductance component at the fundamental $g^{(1)}$ to the conductance component at the second harmonic $g^{(2)}$ by simply substituting $V = V_s \cos \omega_s t$ into (16) and (18) and expanding (16) and (18) with the following result:

$$\frac{g^{(1)}}{g^{(2)}} = \frac{\Delta i_s}{i_s} \cdot \frac{I_1(\alpha V_0)}{I_2(\alpha V_0)}, \quad \text{for } i_s \text{ unbalance} \quad (19)$$

and

$$\frac{g^{(1)}}{g^{(2)}} = \frac{\Delta \alpha}{\alpha} \cdot \frac{I_1(\alpha V_0)}{I_2(\alpha V_0)}, \quad \text{for } \alpha \text{ unbalance.} \quad (20)$$

In Fig. 2 the ratio $g^{(1)}/g^{(2)}$ is plotted versus $\Delta \alpha/\alpha$ or $\Delta i_s/i_s$. It can be seen that if one were to operate under LO "starved" conditions ($V_{LO} < 0.1$ V) the effect of the unbalance can be severe. However, for typical LO voltages of 0.7 V or greater, (19) and (20) reduce approximately to

$$\frac{g^{(1)}}{g^{(2)}} = \frac{\Delta i_s}{i_s}, \quad \text{for } i_s \text{ unbalance} \quad (21)$$

and

$$\frac{g^{(1)}}{g^{(2)}} = \frac{\Delta \alpha}{\alpha}, \quad \text{for } \alpha \text{ unbalance.} \quad (22)$$

Thus the percentage unbalance in either i_s or α translates directly into the percentage of $g^{(1)}$ as compared to $g^{(2)}$. This does not mean, however, that the ratio of undesired fundamental conversion loss to the desired second-harmonic conversion loss will be directly proportional to $g^{(1)}/g^{(2)}$, since the conversion loss will depend on exactly what load impedance is presented to the diode at the fundamental mixing frequency. To accurately predict the fundamental conversion loss, detailed characterization of the embedding circuit at the fundamental mixing frequency would be necessary.

The second-harmonic mixing conversion loss may be estimated by noting (Fig. 1) that the pulse duty ratio (PDR) [6] for the antiparallel diode pair will be essentially double that attainable at the fundamental LO frequency since the period at the second harmonic is halved. Referring to Barber's paper [6, fig. 4], a doubling of

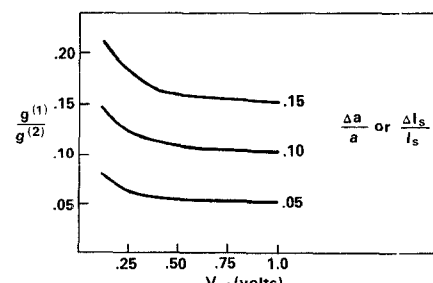


Fig. 2. Unbalance versus LO power.

the PDR (for the matched image case) from a typical value of 15 percent to 30 percent represents a degradation of approximately 1.5 dB for the second-harmonic conversion loss as compared to fundamental mixing. Such an estimate, of course, is only approximate since: 1) the conversion loss depends on the terminations presented to the diode at the various frequencies, and 2) the cited curve from Barber's paper is for an ideal diode with no series resistance or shunt junction capacitance. Nonetheless, such an estimate is useful in assessing the merits of the harmonic mixing approach as compared to fundamental mixing.

It should also be pointed out that image enhancement techniques can be used with an antiparallel diode pair mixer to improve conversion loss. Such an experiment is described in Section III of this paper, and also in a recent paper by Schneider [7]. Schneider has investigated an image enhanced stripline mixer with a very similar diode configuration and achieved a conversion loss = 3.2 dB at 3.5 GHz.

The degradation of receiver noise figure due to LO noise sidebands is also reduced in even harmonic mixing (m even, $n = 1$) in an antiparallel diode pair as shown in Fig. 3. LO noise sidebands (f_{NL} and f_{NH}) whose separation from the LO (f_{LO}) equals the IF (f_{IF}) generate IF noise which only circulates within the diode loop when they mix fundamentally with the LO. Second-harmonic mixing of these noise sidebands with the virtual LO ($2f_{LO}$) produces noise which is not within the IF amplifier passband. Like a conventional balanced mixer, of course, the degree of suppression is affected by the balance between the diodes.

Finally, the circuit has inherent self-protection against large peak inverse voltage burnout since a reverse biased junction is always in parallel with a forward biased junction. This limits the maximum reverse voltage excursion to a value much less than the reverse breakdown voltage of the diodes.

III. EXPERIMENTAL INVESTIGATION

In order to verify many of the predicted characteristics, an antiparallel pair of GaAs Schottky barrier diodes were shunt mounted across a slot line. A 3-GHz LO input and a 4-GHz low-level signal were impressed at the slot line input. A photograph of the output spectrum is shown in Fig. 4. Note that the output at $3f_{LO}$ is much greater than that at $2f_{LO}$, and the absence of fundamental mixing products, $f_s - f_{LO}$ and $f_s + f_{LO}$, and the relatively large 2-GHz IF output due to second-harmonic mixing ($2f_{LO} - f_s$).

In another experiment, an existing microstrip mixer was modified to accomodate a series-mounted antiparallel diode pair (see Fig. 5) so as to evaluate second-harmonic mixing at 12 GHz using a 7-GHz LO. A measured curve of the total circuit conversion loss (including the insertion loss of the bandpass and low-pass filters and microstrip-to-coaxial line transitions ≈ 2 dB) as a function of fundamental LO drive is shown in Fig. 6. Although no attempt was made to optimize the signal and IF impedance matches, the 8-dB total conversion loss was comparable to that obtained by fundamental mixing at 12 GHz.

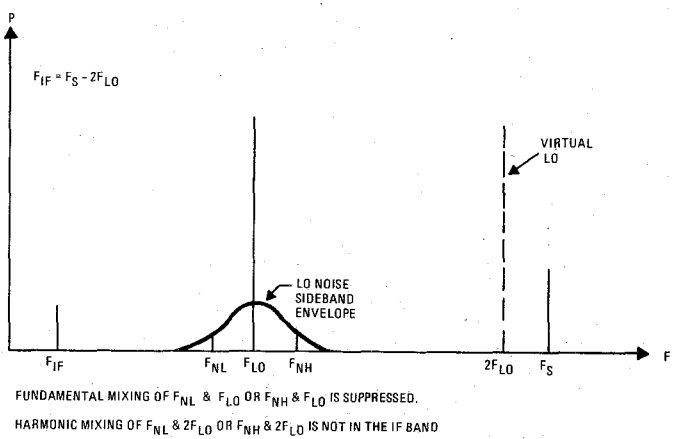


Fig. 3. Noise sideband mixing products.

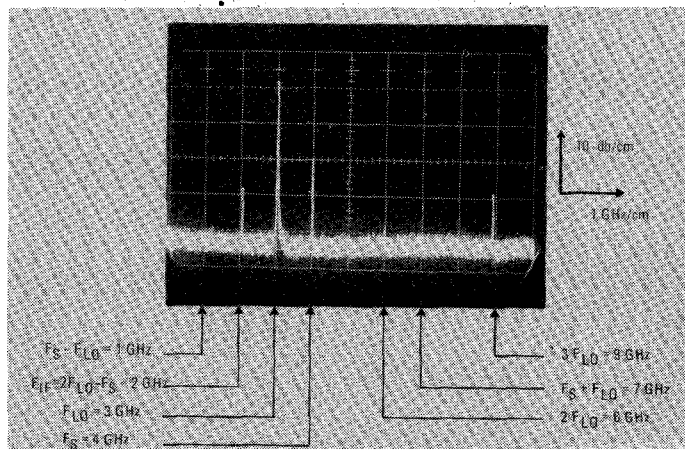


Fig. 4. Power versus frequency for slot line mixer.

An experiment was also conducted into image enhanced harmonic mixing using the circuit shown in Fig. 7. This circuit was originally designed for fundamental image enhanced mixing at the following frequencies [8]:

signal: $f_s = 9.5$ GHz

LO: $f_0 = 8.5$ GHz

IF: $f_{IF} = 1.0$ GHz

In order to modify the circuit for the harmonic mixing experiment, a second diode was mounted antiparallel fashion across the first diode and the following frequencies were applied:

LO: $f_0 = 4.25$ GHz

signal: $f_s = 9.5$ GHz

IF: $f_{IF} = 1.0$ GHz

The LO was injected via a directional coupler since the resonant ring would only pass a narrow range of frequencies about 8.5 GHz. The measured performance of this mixer is shown in the table below.

Fundamental mixing conversion loss	$f_s - f_{LO} = 5.25$ GHz	>45 dB
Harmonic image enhanced mixing conversion loss	$f_s - 2f_{LO} = 1.0$ GHz	< 5 dB
LO harmonic suppression	$2f_{LO} = 8.5$ GHz	>50 dB

For comparison, the measured fundamental image en-

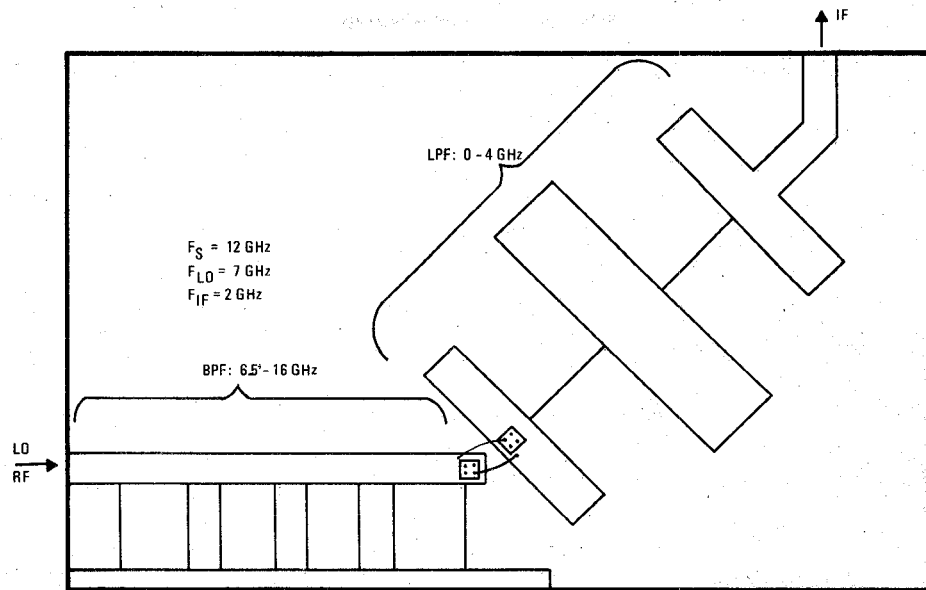


Fig. 5. X-band MIC harmonic mixer layout.

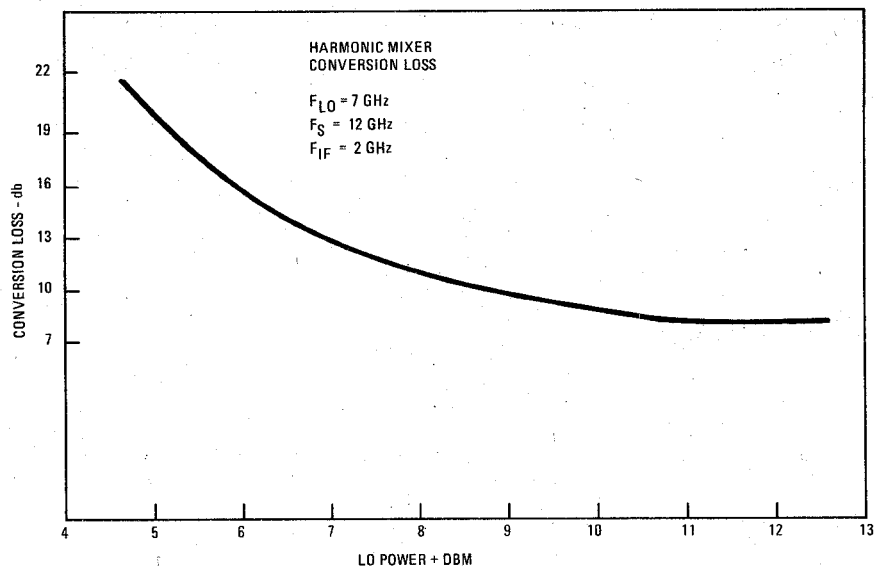


Fig. 6. Conversion loss versus LO power for MIC mixer.

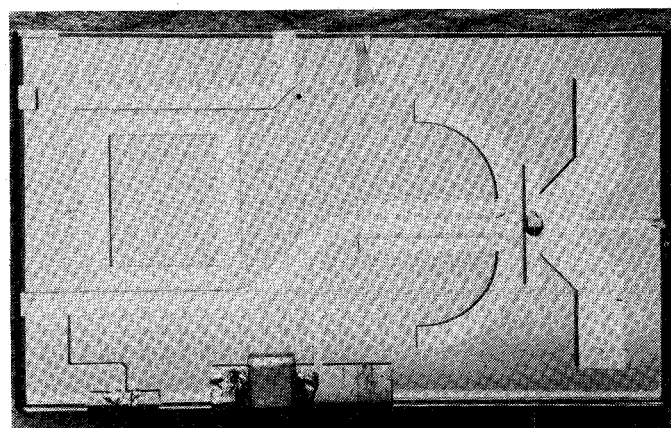


Fig. 7. Image enhanced harmonic mixer.

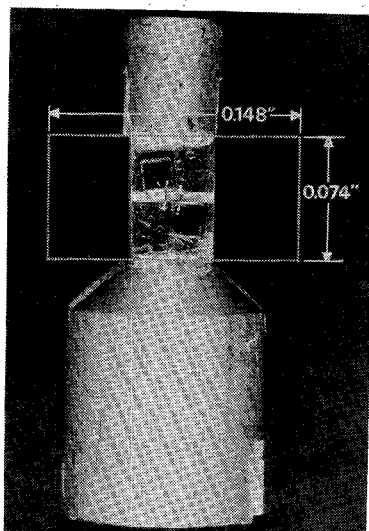


Fig. 8. Millimeter wave diode cartridge.

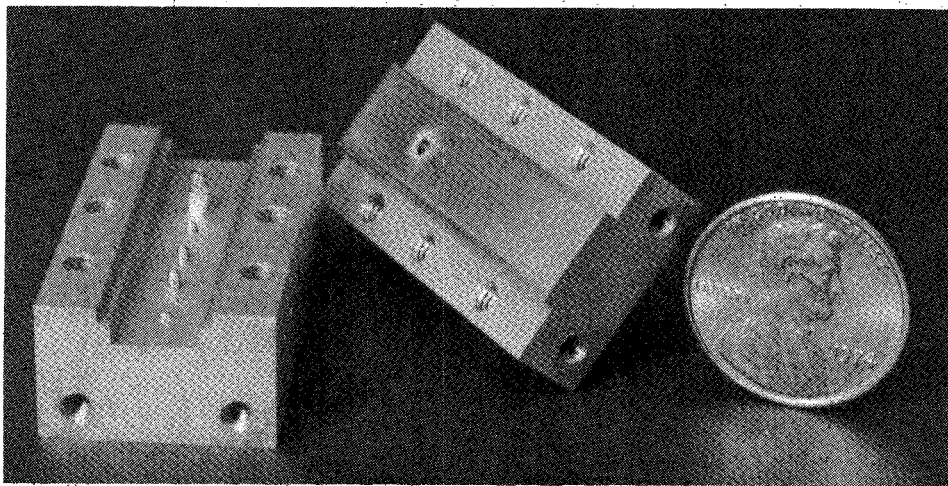


Fig. 9. Waveguide harmonic mixer mount.

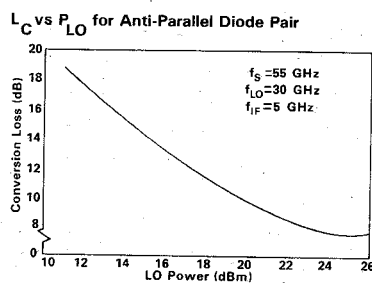


Fig. 10. Conversion loss versus LO power for millimeter wave harmonic mixer.

hanced conversion loss for this circuit before modification was typically 3.5 dB.

A millimeter-wave harmonic mixer was also investigated. The antiparallel diode pair structure designed to be inserted in a WR-15 waveguide is shown in Fig. 8. The Westinghouse developed high-cutoff-frequency GaAs Schottky barrier diodes are mounted on a 0.025-in-thick sapphire substrate which is metallized only on the surface shown. The smaller metallic end cap connects to the center conductor of the coaxial IF output port.

The disassembled mount with cartridge inserted is

shown in Fig. 9. The width of the waveguide has been increased to 0.280 in to allow propagation of the 30-GHz LO. A curve of measured conversion loss versus LO power is shown in Fig. 10. It can be seen that the minimum conversion loss is 8 dB. This diode structure proved to have considerable unbalance, however, as evidenced by the fact that the fundamental conversion loss was also 8 dB. The dc current flowing in the IF circuit was 4 mA versus 0 for the perfect balance case. By way of comparison the dc current in the X-band mixers never exceeded 0.2 mA. It is felt that this unbalance is due to slight differences in the

length of the bonding wires which at this frequency have an inductive reactance of approximately $6 \Omega/0.001$ in of length. Future efforts on this mixer will be concentrated on keeping these wires as short and as equal as possible.

These experiments have confirmed the theoretical predictions of Section II and demonstrated the usefulness of the antiparallel diode pair as a harmonic mixer. Potentially the most useful application of this circuit will be at millimeter wavelengths although careful balancing of the diodes will be required to realize its full potential.

REFERENCES

- [1] M. Cohn, F. L. Wentworth, and J. C. Wiltse, "High-sensitivity 100- to 300-Gc radiometers," *Proc. IEEE*, vol. 51, pp. 1227-1232, Sept. 1963.
- [2] R. J. Bauer, M. Cohn, J. M. Cotton, Jr., and R. F. Packard, "Millimeter wave semiconductor diode detectors, mixers, and frequency multipliers," *Proc. IEEE (Special Issue on Millimeter Waves and Beyond)*, vol. 54, pp. 595-605, Apr. 1966.
- [3] R. Meredith and F. L. Warner, "Superheterodyne radiometers for use at 70 Gc and 140 Gc," *IEEE Trans. Microwave Theory Tech.*, vol. MTT-11, pp. 397-411, Sept. 1963.
- [4] F. A. Benson, *Millimetre and Submillimetre Waves*. London, England: Iliffe Books, 1969, ch. 22.
- [5] M. Cohn, J. E. Degenford, and B. A. Newman, "Harmonic mixing with an anti-parallel diode pair," in *1974 MTT Int. Symp. Dig.*, pp. 171-172, June 12-14, 1974.
- [6] M. R. Barber, "Noise figure and conversion loss of the Schottky barrier mixer diode," *IEEE Trans. Microwave Theory Tech.*, vol. MTT-15, pp. 629-635, Nov. 1969.
- [7] M. V. Schneider, "Harmonically pumped stripline down converter," presented at the European Microwave Conf., Montreux, Switzerland, Sept. 10-13, 1974.
- [8] J. B. Cahalan, J. E. Degenford, and M. Cohn, "An integrated X-band, image and sum frequency enhanced mixer with 1 GHz IF," in *1971 IEEE Int. Microwave Symp. Dig.* (Washington, D. C.), May 17-19, 1971.

Effect of Temperature on Device Admittance of GaAs and Si IMPATT Diodes

YOICHIRO TAKAYAMA, MEMBER, IEEE

Abstract—The effect of temperature on the small-signal admittance of IMPATT diodes with uniformly doped and high-low doped (Read) structures is investigated experimentally and theoretically. Small-signal admittance characteristics of X-band Si p^+-n-n^+ , GaAs $M-n-n^+$ (Schottky-uniform), and GaAs $M-n^+-n-n^+$ (Schottky-Read) IMPATT diodes are measured at various junction temperatures for different dc current levels. Small-signal analysis is performed on GaAs IMPATT diodes of uniformly doped and high-low doped structures, and the calculated results on temperature dependence of the device admittance are compared with the experimental results. Reasonable agreement is found between theory and experiment. It is shown that GaAs IMPATT diodes are superior to Si diodes in admittance temperature characteristics and that the uniformly doped structure has a small admittance temperature coefficient in magnitude, compared to the high-low doped structure. It is also shown by calculation that the admittance temperature coefficient of a punch-through diode is small in magnitude, compared to that of a non-punch-through diode.

I. INTRODUCTION

RECENTLY, Si and GaAs IMPATT diodes with various structures have been developed. In their applications to microwave oscillators and amplifiers, temperature variation of operating characteristics, such as frequency, power, phase, and noise, is a serious problem. The tem-

perature dependence of the device admittance of IMPATT diodes is a fundamental factor for assessing the temperature characteristics of IMPATT oscillators and amplifiers. Temperature dependence of small-signal admittance of IMPATT diodes has been calculated by several authors for restricted structures and operating conditions [1]-[4]. However, those previous works are fragmental and do not present a sufficiently detailed picture. Furthermore, no experimental investigation to determine temperature effect on IMPATT diode admittance has been reported so far.

The purpose of this paper is to present a basic understanding of temperature effect on small-signal admittance of IMPATT diodes with various structures, and to provide an available guide for network and device design, considering the temperature effect. Small-signal admittance characteristics of X-band Si p^+-n-n^+ , GaAs $M-n-n^+$ (Schottky, uniformly doped), and GaAs $M-n^+-n-n^+$ (Schottky-Read) IMPATT diodes were measured at various junction temperatures for different dc current levels. Small-signal analyses of GaAs IMPATT diodes with the uniformly doped and high-low doped (or Read-type) structures were performed and the calculated results on the temperature characteristics of GaAs IMPATT diode admittance are compared to the experiments. Reasonable agreement was found in the temperature dependence of the device admittance between theoretical and experimental results.

Manuscript received August 22, 1974; revised March 20, 1975. The author is with Central Research Laboratories, Nippon Electric Company, Nakahara-ku, Kawasaki, Japan.